Neural Network Classification of Gamma-Ray Bursts

Andreu Balastegui[1], Pilar Ruiz-Lapuente[1,2] and Ramon Canal[1,3]

[1]*Departament d'Astronomia i Meteorologia, Universitat de Barcelona, Martí i Franqués 1, Barcelona 08028, Spain*

[2]*Max-Planck-Institut für Astrophysik, Karl-Schwarzschild-Strasse 1, 85740 Garching bei München, Germany*

[3]*Institut d'Estudis Espacials de Catalunya, Nexus Building, Gran Capità 2-4, Barcelona 08034, Spain*

abalaste@am.ub.es; pilar@am.ub.es; ramon@am.ub.es

Abstract. **From a cluster analysis it appeared that a three-class classification of GRBs could be preferable to just the classic separation of short/hard and long/soft GRBs (Balastegui et al., 2001). A new classification of GRBs obtained via a neural network is presented, with a short/hard class, an intermediate-duration/soft class, and a long/soft class, the latter being a brighter and more inhomogenous class than the intermediate duration one. A possible physical meaning of this new classification is also outlined.**

Classical Classification

The existence of two different classes of gamma-ray bursts (GRBs) has been known since 1993 (Kouveliotou et al.). The bimodal distribution of the duration logarithms defined the separation between long (T_{90} > 2 s) and short (T_{90} < 2 s) GRBs. It was also known that short GRBs have harder spectra than long GRBs. That is the classical separation between short/hard and long/soft GRBs. Horváth (1998) made the first step towards a three-class classification of GRBs by fitting the duration distribution with three gaussians. However, these firsts classifications were unable to assign individual bursts to definite classes: they only defined limiting durations, while short and long GRBs durations are overlapped.

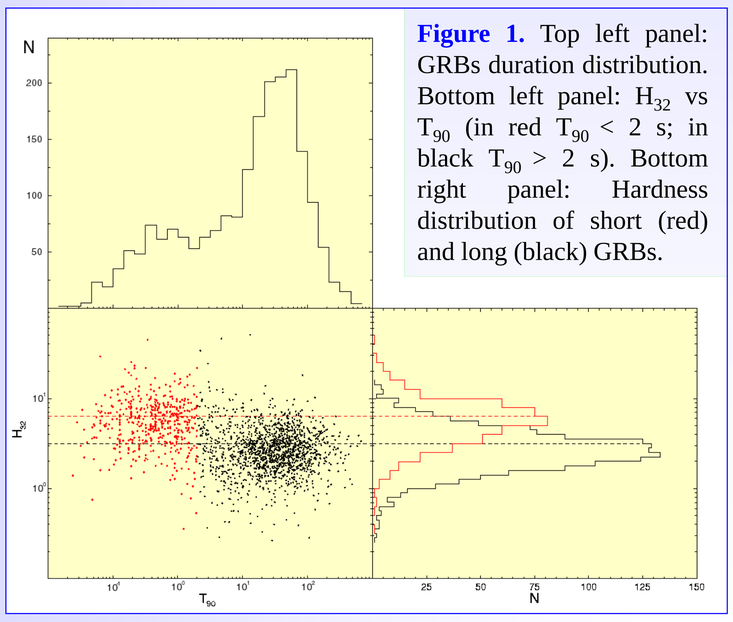

Figure 1. Top left panel: GRBs duration distribution. Bottom left panel: H_{32} vs T_{90} (in red T_{90} < 2 s; in black T_{90} > 2 s). Bottom right panel: Hardness distribution of short (red) and long (black) GRBs.

Cluster Analysis

Duration is not the only relevant characteristic of GRBs, and the BATSE catalogue supplies up to nine physical quantities intrinsic to the burst: four fluences (corresponding to the four energy channels: Ch#1 25-50 KeV; Ch#2 50-100 KeV; Ch#3 100-300 KeV; Ch#4 > 300 KeV), three peak fluxes (corresponding to the three time-scales of integration: 64, 256 and 1024 ms) and two durations (T_{50} and T_{90}). In addition, here we use the hardness ratio H_{32} and V/V_{max}. A cluster analysis is applied to the logarithms of these 11 quantities. That is an agglomerative hierarchical clustering method, which starts from n points separated in the 11-dimensional space and that will be grouped until one ends up with only one cluster. The method looks for clusters with minimum variance among objects belonging to that group and with maximum variance between clusters. Figure 2 shows the dendrogram with the last six levels of clustering. We see that the most important increase of the variance occurs when joining group 3 with group 2, telling us that we have merged two groups with different characteristics. There is also an important rise in variance when merging cluster 2 with cluster 1. This analysis favours the three-class classification over the classical two-class classification.

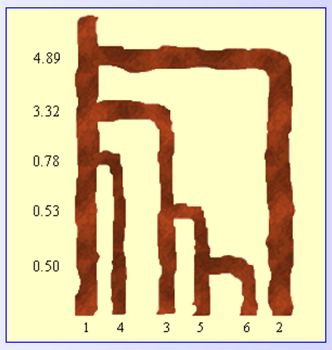

Figure 2. Dendrogram of the 11-dimensional analysis. The numbers at the bottom of the diagram are identifiers of the groups, and those at the left show the inner variance of the groups. For instance, when merging group 6 with group 5 the variance of the cluster is 0.50.

Neural Networks

One step beyond cluster analysis is the neural network classification which can handle non-linear relationships. Neural networks are artificial intelligence algorithms that can be used for an automatic and objective classification. We have used the 'Self-Organizing Map' algorithm (Kohonen 1990), a non-supervised algorithm, since we do not want to start from any known classification. Like in the cluster analysis, the entrance parameters will be the logarithms of the same 11 variables. We have to specify to the program the dimension of the output space, and based on the results of the cluster analysis we will run the network two times asking for a two and a three-dimensional output space, grouping thus two or three classes of GRBs.

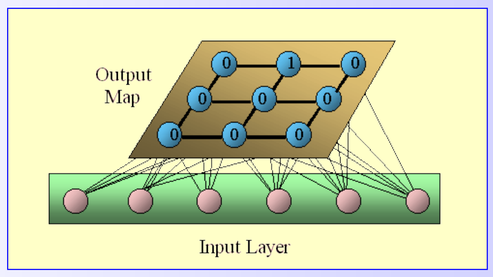

Figure 3. Schematics of a Kohonen 'Self-Organizing Map'.

New Classification

Table 1 summarizes the characteristics of the two-class and three-class classifications of the neural network. As it can be seen the two-class classification recovers the classical short/hard and long/soft GRBs, but now we are able to classify individual bursts in the overlapping region. It is surprising that classical short GRBs have durations up to 100 s. In the three-class classification, the new class 3-II is composed by the longer and softer bursts from class 2-I, and by the shorter bursts from class 2-II. This new class of intermediate duration has the same hardness as the long duration class. In contrast they have different fluences, peak fluxes and rather different values of $\langle V/V_{max} \rangle$. All classes derived from the neural network are compatible with isotropy, as seen from the values of the dipole ($\langle \cos\theta \rangle$), and quadrupole ($\langle \sin^2 b - 1/3 \rangle$) moments.

Table 1. Characteristics of the neural network GRBs classification. T_{90} is in units of s, P_{1024} in units of photon cm^{-2} s^{-1}, and F_{total} in units of 10^{-6} erg cm^{-2}.

Class	N	$\langle T_{90} \rangle$	$\langle H_{32} \rangle$	$\langle V/V_{max} \rangle$	$\langle P_{1024} \rangle$	$\langle F_{total} \rangle$	$\langle \cos\theta \rangle$	$\langle \sin^2 b - 1/3 \rangle$
2-I	685	6.24 ± 0.50	5.50 ± 0.18	0.288 ± 0.015	0.94 ± 0.04	1.44 ± 0.09	+0.002 ± 0.024	−0.005 ± 0.012
2-II	914	63.5 ± 2.3	3.12 ± 0.05	0.159 ± 0.008	3.82 ± 0.22	25.1 ± 2.0	−0.024 ± 0.021	+0.001 ± 0.010
3-I	531	3.05 ± 0.34	6.20 ± 0.22	0.287 ± 0.017	0.81 ± 0.04	1.13 ± 0.07	−0.003 ± 0.027	−0.014 ± 0.014
3-II	341	25.0 ± 1.4	3.05 ± 0.10	0.307 ± 0.019	1.25 ± 0.08	2.82 ± 0.16	−0.012 ± 0.033	+0.009 ± 0.016
3-III	727	71.8 ± 2.8	3.15 ± 0.05	0.123 ± 0.008	4.51 ± 0.28	30.8 ± 2.5	−0.022 ± 0.023	+0.003 ± 0.012

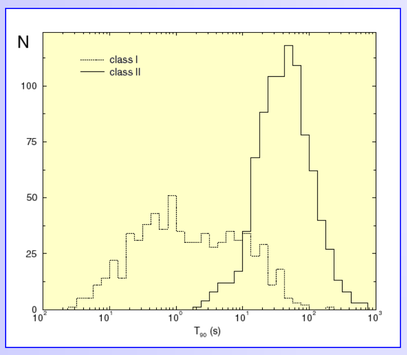

Figure 4. Two class neural network duration distribution.

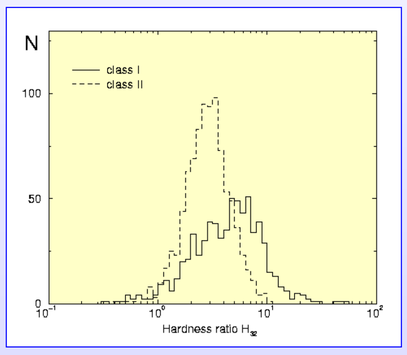

Figure 5. Two class neural network hardness distribution.

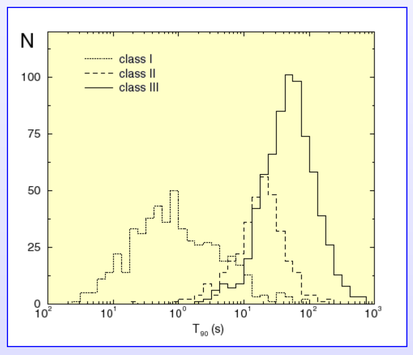

Figure 6. Three class neural network duration distribution.

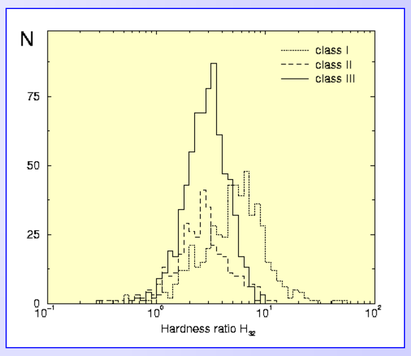

Figure 7. Three class neural network hardness distribution.

Hardness evolution

$\langle V/V_{max} \rangle$ gives a measure of the maximum redshift of a sample of GRBs, the lower its value the deepest the population being, so class 3-III GRBs are the farthest ones. Figure 8 shows that classical long-duration GRBs are harder the farther away they are produced. That evolution, however, only holds for class 3-III GRBs of the new classification, as it can be seen in figure 9. GRBs produced from collapsars are expected to take place at very long distances and may possess such evolution with distance, that making them good candidates to produce class 3-III GRBs. On the other hand, compact-object mergings are expected to happen at shorter distances and lack such evolution, that making them good candidates to produce classes 3-I and 3-II GRBs.

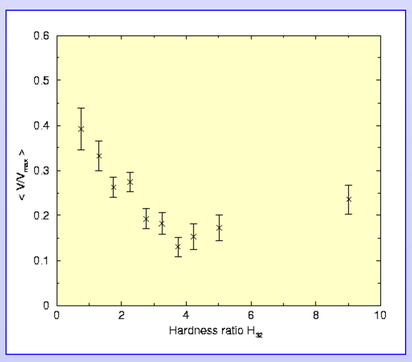

Figure 8. $\langle V/V_{max} \rangle$ vs hardness for GRBs with T_{90} > 2 s. The correlation between these two variables is clearly seen.

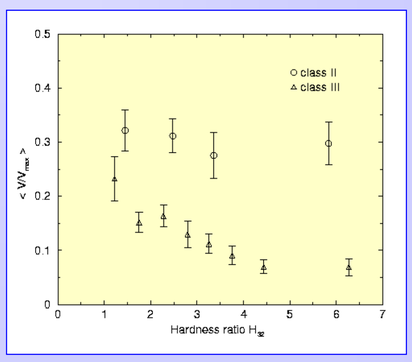

Figure 9. $\langle V/V_{max} \rangle$ vs hardness for class 3-II (circles) and 3-III (triangles). The correlation between these two variables is now only present for class 3-III.

Bibliography

Balastegui A., Ruiz-Lapuente P., Canal R., 2001, MNRAS, 328, 283
Horváth I., 1998, ApJ, 508, 757
Kohonen T., 1990, IEEC Proc., 78, 1464
Kouveliotou C. et al., 1993, ApJ, 413, L101